Electrochemical behaviour of nanostructured bioglass®/alginate composite coating on magnesium alloy by electrophoretic deposition for orthopaedic application

A.H. Azizi, S.R. Allahkaram*

School of Metallurgy and Materials Engineering, College of Engineering, University of Tehran, Tehran, Iran.

*Corresponding author email: akaram@ut.ac.ir

ABSTRACT

The present work aimed to develop the anodic electrophoretic deposition (EPD) of sodium alginate/nano-Bioglass® (Na-Alg/nBG) bioactive nanocomposite coatings on Mg-Zn-Ca alloy without any previous surface pre-treatment (other than polishing). In comparison with other alloys, such as stainless steel or titanium, the density and elastic modulus of magnesium are similar to those of natural bone, and corrosion products of Mg-Zn-Ca alloy are not harmful to the patient body. Alginate is an anionic natural polysaccharide which, due to its low toxicity and biocompatibility, has been studied for different biomedical applications. Through the presence of Bioglass® particles in the coatings, mechanical properties are advanced by increasing adhesion to the substrate and also increases the formation of hydroxyapatite after immersion in simulated body fluid (SBF). A stable water/ethanol EPD suspension was used to produce composite nBG/Alg coating for potential biomedical applications. nBG contents (3 g/L) were studied for a constant concentration of sodium alginate (10 g/L); DC voltage and deposition times varied between 3-20 V and 10-60 seconds, respectively. It has been revealed how electrophoretic deposition (EPD) occurs on the magnesium alloy surface. The coatings composition was analyzed by X-ray diffraction (XRD) and Fourier-transform infrared spectroscopy (FTIR) and the surface of the coatings was studied with field emission scanning electron microscopy (FESEM). For investigating corrosion protection of bioactive coatings, polarization and electrochemical impedance spectroscopy (EIS) tests were used; samples were immersed in simulated body fluid (SBF) at 37°C and results were compared with the bare uncoated Mg-Zn-Ca alloy. The present work confirmed that electrophoretic deposition is a practical method for the co-deposition of Bioglass® nanoparticles and Na-Alg that can be used to produce a wide range of magnesium alloy coatings with tailored microstructures and surfaces with biomedical applications.

Keywords: Electrophoretic deposition; Bioglass®; Alginate; Magnesium alloy; Composite coating.

1. Introduction

Researchers are seeking to develop methods for changing the surface properties of metallic prostheses (Ti-based alloy, stainless steel, Mg-based alloy, CoCr alloy) because of the inherent biocompatible character of these metals and the possibility of ions releasing from the surfaces, which can result in interfacial loosening after implantation [1-4]. Stainless steel and titanium alloys are currently the most commonly used metallic alloys for implants [5]. Nevertheless, these alloys do not always react well with the body, which can result in inflammation after implanting them. Additionally, the formation of fibrous tissue surrounding the implant could enclose the implant [6], and non-compatible ions could be released into the body [7]. The investigation has been conducted on improving osseointegration and ensuring

binding affinity to human tissue by modifying implant surfaces with bioactive materials [8,9].

There is considerable interest in using magnesium alloys as a biomaterial for biodegradable implants [10]. Because Mg alloys are biodegradable, the patient would not need to undergo a second surgical procedure after implantation [11]. Magnesium has the highest strength-to-weight ratio of all metals as well as its compressive yield strength and Young's modulus are similar to those of natural bone. Moreover, Mg is essential for human metabolism, and excess is excreted through urine [12]. Magnesium, from the mechanical and physical perspective, such as Young's modulus, yield strength, tensile strength, density, and thermal expansion coefficient has all these attributes that make it superior to most other metal alloys for orthopedic applications [13]. However, Mg alloys are limited because physiologic conditions make them corrode easily, leading to the release of hydrogen into the atmosphere upon magnesium breakdown, resulting in inflammation of the tissue nearby. In the physiological environment, magnesium alloys can be very active, so the absence of a barrier layer may result in an accelerated magnesium ions release and reduced implant mechanical stability [14,15]. There have been several solutions developed in three areas to deal with magnesium's disadvantages [16]. First, the development of alloys with lower degradation rates. This route is better than pure metal, but the results are often inadequate [16]. The addition of Zn and Ca decreases the corrosion potential of the magnesium alloy and the in-vitro degradation rate of the Mg alloy; The degradation of Mg-Zn-Ca alloys was decreased by a protective layer of $Mg(OH)_2$ and Mg/Ca phosphates. ZX504 alloy has a superior mechanical and chemical stability (in SBF solution) than other available magnesium alloys after 30 days. Furthermore, zinc and calcium increase the corrosion potential of magnesium alloy and reduce in-vitro degradation rates in simulated body fluid. Also, compared to other alloys, zinc and calcium-containing magnesium alloys show good biocompatibility in in-vitro cytotoxicity tests [17-19]. Secondly, it is possible to modify the microstructure of the material (grain size and phase distribution) [20,21]. A third technique, which has been widely studied, is coating Mg-Zn-Ca alloy with bioactive materials [22,23]. Accordingly, magnesium-based alloys containing calcium and zinc (i.e. ZX504) are the better choice for orthopedic application than other available magnesium alloys.

Bioactive glass (BG), particularly 45S5 (45wt% SiO_2, 24.5wt% CaO, 24.5wt% Na_2O, 6wt% P_2O_5) is investigated in biomedical applications because it can form a layer of hydroxyapatite on its surface that forms a strong contact with bone [24]. Pure bioactive glass coatings on metallic substrates must be sintered to achieve adequate adhesion; however, this may damage the substrate's properties; furthermore, the brittle nature of BG makes it prone to crystallizing and microcracking during high-temperature treatments [25,26]. In general, polymeric binder addition increases the affinity of BG particles to metallic substrates, eliminating the need for undesirable high-temperature treatments [9,27]. Additionally, the polymer coating effectively controls the rate of dissolution of the BG and facilitates the adsorption of proteins. Alginate is a polymer that can be used for this purpose; Alginate is a water-soluble natural anionic polysaccharide that is usually derived from seaweed and is highly investigated for its potential in biosensors, drug delivery, tissue engineering and other biomedical applications due to its biocompatibility, low toxicity and cost-effectiveness [28]. In light of these findings, it seemed that Alg/BG nanocomposite coatings contain bioactive properties and could be used in dental and orthopaedic implants, as well as scaffolds for bone tissue [9].

Electrophoretic deposition (EPD) is one of the more popular coating techniques in the past few decades because of its cost-effectiveness, high deposition rate, room temperature operation, and controllable thickness. EPD is a colloidal technique, which moves charged particles or molecules to electrodes by introducing an electric field into a suspension. This process enables the deposit of a wide range of materials, including organic, inorganic, or composite materials, as well as polymers, proteins and enzymes [31,32].

The purpose of this study was to develop alginate-based composite coatings incorporating BG nanoparticles as inorganic phases on magnesium alloy substrate by electrophoretic deposition. The deposition parameters (concentration of suspension, deposition voltage and deposition time) and stability of suspension were investigated. Coating compositions have been investigated with X-ray diffraction (XRD) and field emission scanning electron microscope (FESEM) analysis. We also measured the electrochemical behavior of the

coated substrates by obtaining polarization curves and electrochemical impedance spectroscopy to determine the protective effect of the coatings on the corrosion behavior of the Mg-Zn-Ca substrates.

2. Experimental details
2.1. Substrate preparation

Sheets of the Mg-5wt% Zn-0.4wt% Ca (ZX504) alloy with dimensions of 25×15×2 mm, were prepared with the alloy's chemical composition shown in Table 1. Wet-abrasion was performed with SiC paper up to 1000-grit, followed by ultrasonically cleaning in ethanol for 10 minutes and drying in warm air.

2.2. Suspension preparation

The following steps have been taken to prepare a suspension of glass particles in alginate. A solution of sodium alginate (Loba Chemie) was dissolved in deionized water under magnetic stirring for 1 hour and sonicated for 10 minutes thereafter. In order to inhibit the electrolysis of water, ethanol was added to the suspension while it was being stirred continuously (the ratio of water to ethanol was 60:40). Nano bioactive glass (45S5 Bioglass®, nBG) with the typical composition (wt%): 45% SiO_2, 24.5% CaO, 24.5% Na_2O and 6% P_2O_5 used. After the nBG powder was gradually added to the alginate suspension, which was stirred for 1 hour of magnetic stirring then 20 minutes of ultrasonication. The final concentrations of alginate and nBG were 10 g/L and 3 g/L

respectively, with pH of 11.8±0.1 in the suspension.

2.3. Electrophoretic deposition

To prevent particle sedimentation and coagulation, the suspension was magnetically stirred before each deposition process. As sodium alginate (Na-Alg) decomposes, it forms Alg^- and the hydrolysis of water decreases pH at the anode surface; So, anodic EPD is accomplished through Alg^- electrophoresis followed by low pH neutralization at the anode interface, as described elsewhere [28]. With a stainless steel counter electrode, EPD coatings were deposited on magnesium alloy substrate as anode. A distance of 10 mm was fixed between the electrodes. Different times of deposition (10-60 s) and potentials (3-20 V) were tested to identify optimal EPD parameters; resulting in 15 V and 15 s as best deposition parameters. Fig. 1 illustrates a schematic of the electrophoretic deposition process from Alg/nBG solution. Two-layer EPD coatings were applied in order to compare the characterization of one-layer and two-layer coatings. Therefore, after the anode has been deposited, it was gently removed and held at room temperature for 24 hours to dry before repeating EPD.

2.4. Characterization and electrochemical measurements

Secondary electron (SE) field emission scanning electron microscopy (FESEM) with MIRA3TESCAN-MXU was applied to analyze

Table 1- Chemical composition (wt%) of the ZX504

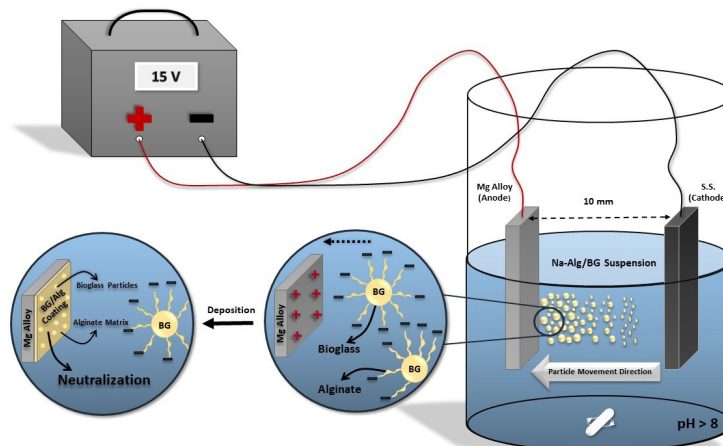| Zn	Ca	Cu	P	Fe	Mn	Al	Mg
4.731	0.365	0.028	0.005	< 0.001	< 0.001	< 0.001	Balance

Fig. 1- Schematic illustration of the EPD mechanism of Na-Alg/BG particle composite coating.

sample surfaces. Fourier transform infrared spectroscopy (Bruker Optik GmbH, Ettlingen, Germany) was used to recognize the chemical groups of both alginate and bioactive glass and verify their coating presence. X-ray diffraction (XRD) was performed to identify bioactive glass phase coating obtained with a Cu Kα radiation in a Philips X′pert Pro PW1730 diffractometer with a working voltage of 40 kV and λ = 1.5405 Å. The analysis was conducted by X′pert High Score Plus.

The coating corrosion performance of the coatings was evaluated by electrochemical impedance spectroscopy (EIS) and polarization measurements using the Solarton-SI1287 potentiostat and Solarton-SI1260 frequency analyzer. Using three electrodes, the working electrode is the coated and uncoated magnesium alloy, the reference electrode is saturated calomel, and the counter electrode is a platinum plate. For all samples, the working electrode's exposure area was considered to be 1.76 cm². In addition, corrosion measurements were carried out on uncoated samples, single-layer coated, and double-layer coated under different voltage and time conditions. In order to be more accurate in measuring corrosion rate, three samples were prepared from each condition. The results of corrosion measurements in all tests were similar. In this paper, in addition to the bare sample, the coated samples that were evaluated for corrosion test were labeled as follows: Single-layer coating 15 V-15 s (A), single-layer 5 V-15 s (B), double layer 15 V-15 s (C). The coatings were immersed in simulated body fluid (SBF) for the purpose of observing any possible changes in corrosion resistance. The temperature of the solution was adjusted to 37 °C and the voltage changes of the samples immersed in the SBF were observed by a voltmeter. When the voltage was displayed it reached a constant value and the open circuit potential (OCP) was obtained; corrosion measurement tests were performed. On average, it took 14 minutes for uncoated samples to reach OCP, and 18 minutes for coated samples.

3. Results and discussion
3.1. Deposition process

The deposition time and electric potential of the process have been varied, in adjustment to achieve homogenous and crack-free coatings. In general, highly elevated potentials (>15 V) and deposition time (>20 s) cause electrolysis water in the electrolyte, which leads to the generation of hydrogen and oxygen on the electrode surfaces, causing bubbles. On the other hand, a low potential (<10 V) and deposition time (<10 s) produce very thin, inhomogeneous coatings that do not adhere to the substrate. Recommended deposition conditions include 15 V and 15 s for suspension with alginate and nBG 10 g/L and 3 g/L respectively. A multilayer approach, with up to 2 layers, has been studied to avoid the formation of bubbles caused by long deposition times, and thus to increase coating thickness. Deposition parameters remained unchanged, followed by a drying period of 24 hours at room temperature between each deposition.

3.2. FESEM observations

Fig. 2 shows FESEM images of the magnesium alloy with composite coating (Alg + nBG) samples at different magnifications. The best quality composite coatings in terms of homogeneity and crack-free coating were obtained at double-layer coating at 15 V and 15 s (as shown in Fig. 2A and B at different magnifications). Alginate serves as a binding agent for bioactive glass nanoparticles incorporated into the coating. During EPD, clusters of 45S5 BG nanoparticles/alginate formed due to the adhesive property of alginate, which, as determined by FESEM, increased the effective size of the particles. The single-layer coating (Fig. 2C), deposited at 15 V and 15 s, shows microcracks throughout the surface caused by hydrogen evolution at the deposition site and shrinkage during drying. According to (Fig. 2D), a higher voltage deposition (30 V) during the same deposition time (15 s) produced numerous microcracks and micropores as hydrogen evolved during deposition and creating bubbles. Also in (Fig. 2E), the effect of lower voltage (5 V) at the constant time (15 s) shows that, despite the absence of cracks and pores in the microstructure, the bioactive glass does not precipitate and the microstructure is free of bioactive glass.

3.3. Coating characterization

As shown in Fig 3a. XRD analysis showed that the coating contained BG; according to data that concluded from X′pert High Score Plus and JCPDS library information, it has been shown that the coating contains 45S5 bioactive glass particles that are deposited on the ZX504 substrate. Also Fig 3b. displays the FTIR spectrum of bioactive glass powders, alginate powder, and alginate-45S5 nanocomposite coatings. FTIR analysis confirmed the presence of alginate: an asymmetric stretching
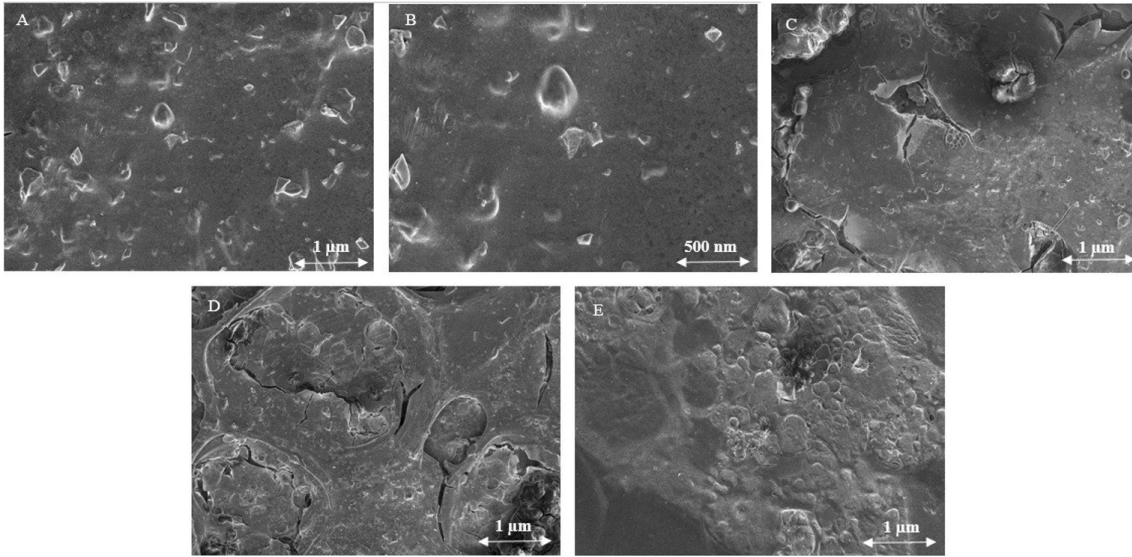
Fig. 2- FESEM images of nBG/Alg coatings on ZX504 Mg alloys at different EPD parameters; double-layer coating at different magnification 15 V-15 s (A and B), single-layer coating 15 V-15 s (C), 30 V-15 s (D) and 5 V - 15 s (E).

vibration and a symmetric stretching vibration COO^- groups at 1600 and 1413 cm^{-1}, respectively, show the presence of alginate [27]. The patterns of bioactive glass powder displays a peak of stretching asymmetrically Si-O at 1050 cm^{-1}, the shoulder at 925 cm^{-1} caused by SiO_{NBO} (non-bonding oxygen), and a peak at about 790 cm^{-1} caused by bending of the Si–O bond [27]. It appears that both alginate and bioactive glass components are present in the spectra of composite coatings, confirming good integration of the glass particles in the polymeric matrix.

3.4. Electrochemical test

EIS (electrochemical impedance spectroscopy) is an effective analysis technique in which a small electrical response (e.g., an electric current or voltage) is applied in varying frequency ranges to affect the metal/electrolyte interface. The electrochemical process is characterized by electrical measurements, which provide information about corrosion, for example about the forming or dissolving of films and local corrosion [33]. For coated and uncoated specimens, Nyquist plots and Bode plots on the experimental medium (SBF at 37 °C) with corresponding open-circuit potentials (OCP) can be seen in Fig. 4. The sample codes are as follows: single-layer coating 15 V-15 s (A), single-layer 5 V-15 s (B), double layer 15 V-15 s (C) and bare Mg alloy. In the first quadrant of the coated samples, two semicircles overlapped (capacitive loop), and in the fourth quadrant, there is also an additional loop (inductive loop).
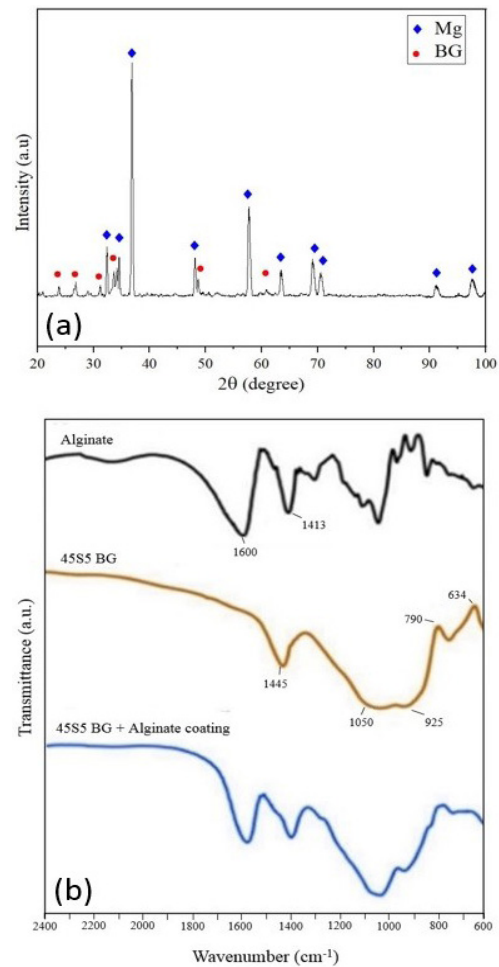

Fig. 3- (a) XRD pattern of the nBG/Alg, and (b) FITR spectra of alginate powder, 45S5 bioactive glass and nBG/Alg coating.

Different corrosion kinetic processes are indicated by the presence of three loops. To obtain more information about what happens at interfaces, EIS data from coated and uncoated specimens were extracted using equivalent circuits (Fig. 4d); table 2. shows the fitting results. The results of the Nyquist plots (Fig. 4a) follow the results of the FESEM results in Fig. 3 which predicts a higher corrosion resistance with double-layer coatings due to fewer cracks and porosities.

Considering ZX504 Mg alloy, R_s indicates solution resistance, R_{ct} signifies charge transfer resistance, and CPE_{dl} represents the capacitance of the double layer at the surface of the electrode and electrolyte. Based on the electrical circuit of the Mg with coatings (Fig. 4d), it was found there was a duplex structure consisting of outer (CPE_1) and inner (CPE_2) sections were observed because of different impedances and phases. R_1 and CPE_1 elements in the equivalent circuit represent the resistance and capacitance of the outer layer (surface defects in the film), in that order. According to R_L and CPE_2, the inner layer's resistance and capacitance are attributed to (dense layers on the metal surface). As well, it appears that the barrier portion of the coatings provided corrosion resistance. Based on the polarization resistance ($R_p = R_1 + R_L + R_{ct}$) measured for each specimen (Table. 2), the double-layer coating deposited at 15 V and 15 s revealed the highest polarization resistance.

Table 2- Corrosion factors are derived from the fitted data of impedance data of ZX504 alloy and substrates with coatings. Single-layer coating 15 V-15 s (A), single-layer 5 V-15 s (B), double layer 15 V-15 s (C)

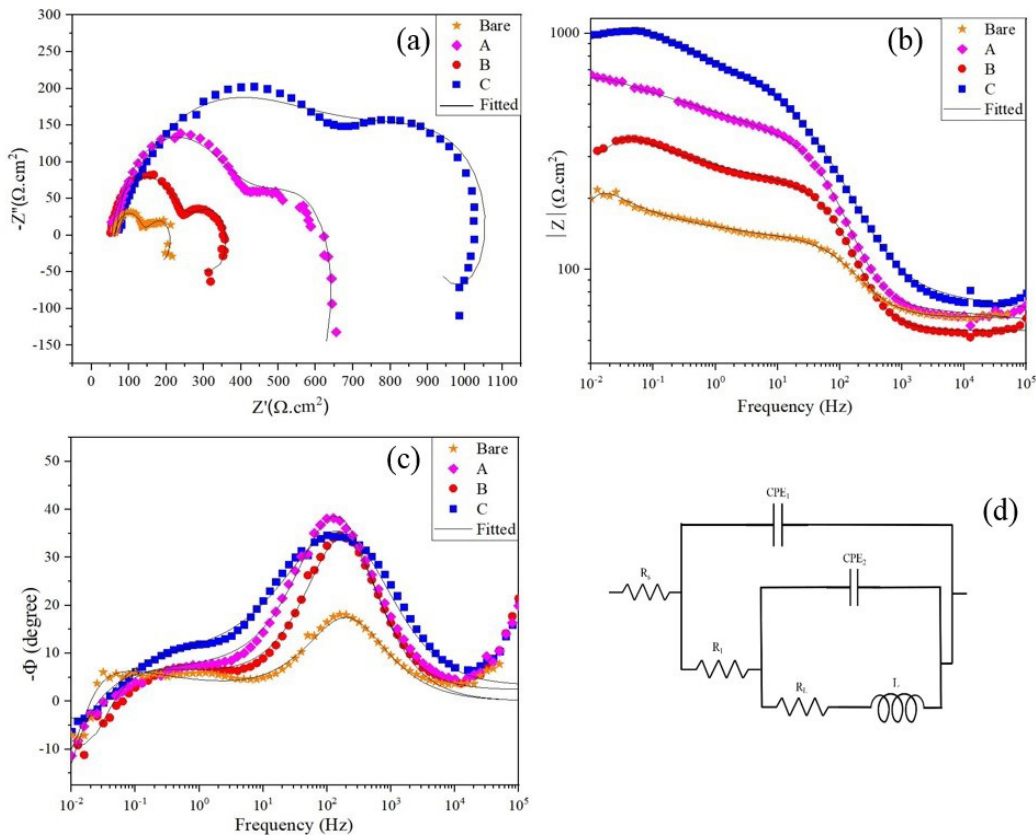| Sample	CPE_1 ($\Omega^{-1}.s^n.cm^{-2}$)	n_1	R_1 ($\Omega.cm^2$)	CPE_2 ($\Omega^{-1}.s^n.cm^{-2}$)	n_2	R_L ($\Omega.cm^2$)	L ($H.cm^2$)
Bare	4.048E-5	0.8648	67.98	2.439E-2	0.4889	17.71	1331
A	1.858E-3	0.7876	91.93	8.118E-6	0.9393	605	2.981E4
B	1.493E-5	0.9471	137.3	7.692E-3	0.283	97.26	1713
C	1.059E-3	0.8521	99.41	1.632E-5	0.7845	2274	2.619E4

Fig. 4- (a) Nyquist, (b) Bode-phase and (c) Bode-|Z| graphs showing coatings and non-coatings measured at 37°C in simulated body fluid, as well as the equivalent circuits derived from the fitting of the impedance measurements of (d) ZX504 and Alg-nBG coated substrate. Single-layer coating 15 V-15 s (A), single-layer 5 V-15 s (B), double layer 15 V-15 s (C).

Fig. 5 presents potentiodynamic polarization measurements using Alg-nBG coatings and uncoated ZX504 Mg alloy in SBF at 37 °C. A summary of corrosion factors (i_{corr}, E_{corr} and Tafel slopes) is provided at Table 3; that single-layer coating 15 V-15 s (A), single-layer 5 V-15 s (B), double layer 15 V-15 s (C). The Tafel extrapolation method was used to extract i_{corr} and E_{corr} data from linear sections of polarization curves. Through this procedure, the linear part of the anodic and cathodic branches is extended, and their collision points indicate the i_{corr} and E_{corr} coordinates and the slope of each branch shows the Tafel slopes. On the ZX504 Mg alloy substrate, the nanocomposite coatings generated lower corrosion current densities (i_{corr}), indicating improved corrosion resistance. After polarization tests, it was determined that among the coated specimens, 15 V-15 s (C) double-layer coating significantly enhanced the corrosion protection of the bare ZX504 alloy. According to the EIS measurements and FESEM observations, these results are accurate.

Fig. 6 shows a schematic illustrating how the samples corroded under uncoated (fig. 6A), single-layer coating (fig. 6B) and double-layer coating (fig. 6C) conditions. Based on the results of EIS and polarization experiments, it appears that the penetration of electrolyte into the substrate is delayed in the presence of double-layer coatings, and therefore corrosion resistance is increased.
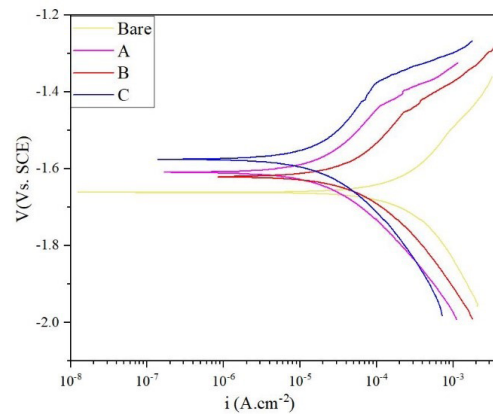

Fig. 5- Potentiodynamic plots for ZX504 Mg alloy and single-layer coating 15 V-15 s (A), single-layer 5 V-15 s (B), double layer 15 V-15 s (C) surfaces with coating in simulated body fluid at 37°C.
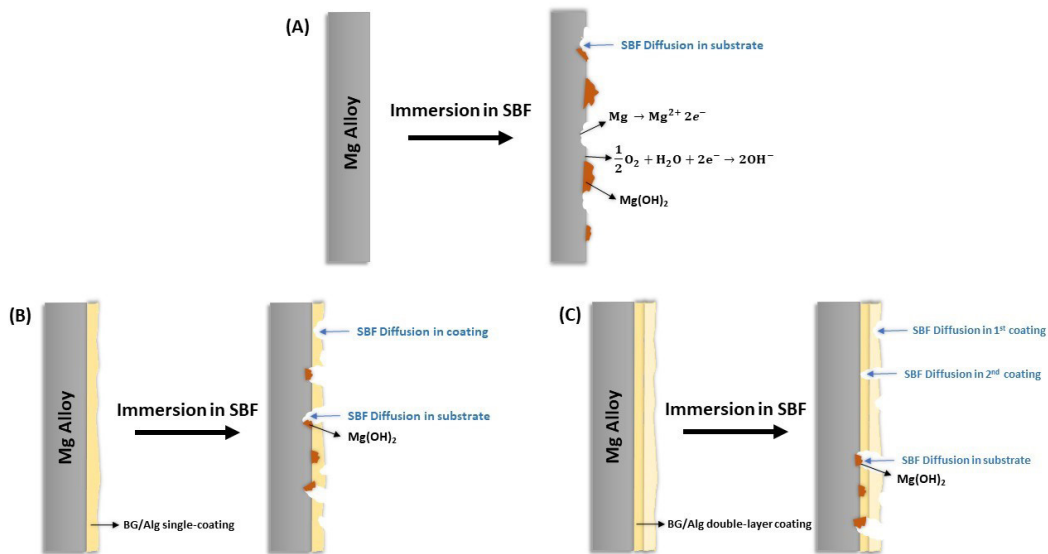

Fig. 6- Schematic illustration of the corrosion mechanism of bare substrate (A), single-layer coating (B) and double-layer coating (C).

Table 3- Results of potentiodynamic data analysis of ZX504 Mg alloy, single-layer coating 15 V-15 s (A), single-layer 5 V-15 s (B), double layer 15 V-15 s (C) surfaces with coating in simulated body fluid at 37°C

Sample	E_{corr} (V)	I_{corr} (A/cm^2)	$-\beta_c$ (mV/dec.)	β_a (mV/dec.)
Bare	-1.661	1.519E-4	141.97	143.13
A	-1.609	1.540E-5	123.88	159.63
B	-1.621	2.910E-5	140.37	103.14
C	-1.575	1.155E-5	100.17	137.31

4. Conclusions

The purpose of this paper, the feasibility study is presented for the corrosion protection of a Mg-Zn-Ca alloy through the application of alginate-45S5 bioactive glass nanocomposite through anodic EPD. For the purpose of avoiding bubble formation and ensuring high colloidal suspension stability during EPD, ethanol/water ratio of 40:60 (vol%) was used to be the optimal solvent ratio and the suspension composition included 10 g/L alginate and 3 g/L 45S5 nano bioactive glass. Voltages 3 to 20 V for the nBG/alginate and deposition time of 10 to 60 s were determined and it was found that 15 V and 15 s were the optimal EPD parameters. The FESEM observation showed that high voltage (>15 V) and deposition time (>20 s) can cause the electrolysis of water, this causes bubbles to form on the electrodes as a result of gas generation. On the other hand, a low potential (<10 V) and deposition time (<10 s) produces very thin, inhomogeneous coatings that do not adhere to the substrate. The presence of nBG in the coatings was proved with XRD investigating and also FTIR analysis of the anodic EPD coatings revealed they contained alginate and nBG. In terms of corrosion behavior in SBF, the difference between the coatings and bare metal in the polarization curves and the EIS observations indicates the double-layer coating displayed greater corrosion resistance against bare metal and single-layer coating. Therefore, biocompatible alginate-bioactive glass nanocomposite coated ZX504 Mg alloy by anodic EPD can be considered as a good candidate for magnesium bioimplant from the corrosion resistance point of view.

References

1. Bagherifard S, Hickey DJ, de Luca AC, Malheiro VN, Markaki AE, Guagliano M, et al. The influence of nanostructured features on bacterial adhesion and bone cell functions on severely shot peened 316L stainless steel. Biomaterials. 2015;73:185-97.
2. Wu G, Ibrahim JM, Chu PK. Surface design of biodegradable magnesium alloys — A review. Surface and Coatings Technology. 2013;233:2-12.
3. Asri RIM, Harun WSW, Samykano M, Lah NAC, Ghani SAC, Tarlochan F, et al. Corrosion and surface modification on biocompatible metals: A review. Materials Science and Engineering: C. 2017;77:1261-74.
4. Li L-H, Kong Y-M, Kim H-W, Kim Y-W, Kim H-E, Heo S-J, et al. Improved biological performance of Ti implants due to surface modification by micro-arc oxidation. Biomaterials. 2004;25(14):2867-75.
5. Chen Q, Thouas GA. Metallic implant biomaterials. Materials Science and Engineering: R: Reports. 2015;87:1-57.
6. Menzies KL, Jones L. The Impact of Contact Angle on the Biocompatibility of Biomaterials. Optometry and Vision Science. 2010;87(6):387-99.
7. Sunderman FW. Carcinogenicity of Metal Alloys in Orthopedic Prostheses: Clinical and Experimental Studies. Toxicological Sciences. 1989;13(2):205-16.
8. Prodana M, Stoian AB, Burnei C, Ionita D. Innovative Coatings of Metallic Alloys Used as Bioactive Surfaces in Implantology: A Review. Coatings. 2021;11(6):649.
9. Chen Q, Cordero-Arias L, Roether JA, Cabanas-Polo S, Virtanen S, Boccaccini AR. Alginate/Bioglass® composite coatings on stainless steel deposited by direct current and alternating current electrophoretic deposition. Surface and Coatings Technology. 2013;233:49-56.
10. Witte F. The history of biodegradable magnesium implants: A review☆. Acta Biomaterialia. 2010;6(5):1680-92.
11. Zhao D, Witte F, Lu F, Wang J, Li J, Qin L. Current status on clinical applications of magnesium-based orthopaedic implants: A review from clinical translational perspective. Biomaterials. 2017;112:287-302.
12. Staiger MP, Pietak AM, Huadmai J, Dias G. Magnesium and its alloys as orthopedic biomaterials: A review. Biomaterials. 2006;27(9):1728-34.
13. Oliver J-AN, Su Y, Lu X, Kuo P-H, Du J, Zhu D. Bioactive glass coatings on metallic implants for biomedical applications. Bioact Mater. 2019;4:261-70.
14. Wan P, Tan L, Yang K. Surface Modification on Biodegradable Magnesium Alloys as Orthopedic Implant Materials to Improve the Bio-adaptability: A Review. Journal of Materials Science & Technology. 2016;32(9):827-34.
15. Salahshoor M, Guo Y. Biodegradable Orthopedic Magnesium-Calcium (MgCa) Alloys, Processing, and Corrosion Performance. Materials (Basel). 2012;5(1):135-55.
16. Heimann RB. Magnesium alloys for biomedical application: Advanced corrosion control through surface coating. Surface and Coatings Technology. 2021;405:126521.
17. Sun Y, Zhang B, Wang Y, Geng L, Jiao X. Preparation and characterization of a new biomedical Mg–Zn–Ca alloy. Materials & Design. 2012;34:58-64.
18. Zhang B, Hou Y, Wang X, Wang Y, Geng L. Mechanical properties, degradation performance and cytotoxicity of Mg–Zn–Ca biomedical alloys with different compositions. Materials Science and Engineering: C. 2011;31(8):1667-73.
19. Shahri Z, Allahkaram SR, Soltani R, Jafari H. Study on corrosion behavior of nano-structured coatings developed on biodegradable as cast Mg–Zn–Ca alloy by plasma electrolyte oxidation. Surface and Coatings Technology. 2018;347:225-34.
20. Johari M, Tabaian SH, Saeedi S. Microstructural Characterization and Investigation on Corrosion Properties of Mg-Zn-RE-Ca Alloy as a Possible Biomedical Implant. Metals and Materials International.

2021.

21. Shahri Z, Allahkaram SR, Soltani R, Jafari H. Optimization of plasma electrolyte oxidation process parameters for corrosion resistance of Mg alloy. Journal of Magnesium and Alloys. 2020;8(2):431-40.

22. Wang HX, Guan SK, Wang X, Ren CX, Wang LG. In vitro degradation and mechanical integrity of Mg–Zn–Ca alloy coated with Ca-deficient hydroxyapatite by the pulse electrodeposition process☆. Acta Biomaterialia. 2010;6(5):1743-8.

23. Hadavi S, Soltani R, Tamjid E, Mehdinavaz Aghdam R. In vitro Corrosion Behavior and Biological Properties of Magnesium-Zinc-Calcium Alloy Coated with Polycaprolactone Nanofibers. Journal of Ultrafine Grained and Nanostructured Materials. 2021 Jun 20;54(1):93-100.

24. Hench LL. Bioceramics. Journal of the American Ceramic Society. 2005;81(7):1705-28.

25. Miola M, Cordero-Arias L, Ferlenda G, Cochis A, Virtanen S, Rimondini L, et al. Electrophoretic deposition of composite coatings based on alginate matrix/45S5 bioactive glass particles doped with B, Zn or Sr. Surface and Coatings Technology. 2021;418:127183.

26. Witecka A, Valet S, Basista M, Boccaccini AR. Electrophoretically deposited high molecular weight chitosan/bioactive glass composite coatings on WE43 magnesium alloy. Surface and Coatings Technology. 2021;418:127232.

27. Cordero-Arias L, Boccaccini AR, Virtanen S. Electrochemical behavior of nanostructured TiO2/alginate composite coating on magnesium alloy AZ91D via electrophoretic deposition. Surface and Coatings Technology. 2015;265:212-7.

28. Sikkema R, Baker K, Zhitomirsky I. Electrophoretic deposition of polymers and proteins for biomedical applications. Advances in Colloid and Interface Science. 2020;284:102272.

29. Besra L, Liu M. A review on fundamentals and applications of electrophoretic deposition (EPD). Progress in Materials Science. 2007;52(1):1-61.

30. Sarkar P, Nicholson PS. Electrophoretic Deposition (EPD): Mechanisms, Kinetics, and Application to Ceramics. Journal of the American Ceramic Society. 1996;79(8):1987-2002.

31. Corni I, Ryan MP, Boccaccini AR. Electrophoretic deposition: From traditional ceramics to nanotechnology. Journal of the European Ceramic Society. 2008;28(7):1353-67.

32. Boccaccini AR, Keim S, Ma R, Li Y, Zhitomirsky I. Electrophoretic deposition of biomaterials. J R Soc Interface. 2010;7 Suppl 5(Suppl 5):S581-S613.

33. Parichehr R, Dehghanian C, Nikbakht A. Preparation of PEO/silane composite coating on AZ31 magnesium alloy and investigation of its properties. Journal of Alloys and Compounds. 2021;876:159995.